

# Finite Element Method Analysis Of Spring Back Of High-Strength Metal SCGA1180DUB While U-Channeling, According To Wall Angle And Die Radius

Samet Karabulut\*, İsmail Esen

Department of Mechanical Engineering, Karabuk University, Karabuk, Turkey

## Research Article

**Received:** 27-Apr-2022, Manuscript No. JOMS-22-61945;

**Editor assigned:** 29-Apr-2022, PreQC No. JOMS-22-61945(PQ);

**Reviewed:** 13-May-2022, QC No. JOMS-22-61945;

**Revised:** 20-May-2022, Manuscript No. JOMS-22-61945(R);

**Published:** 27-May-2022, DOI: 10.4172/2321-6212.10.5.001.

### \*For Correspondence:

Samet Karabulut, Department of Mechanical Engineering, Karabuk University, Karabuk, Turkey

**E-mail:** sametkarabulut@yahoo.com

**Keywords:** Rare-earth hexaboride; Lattice constant; PDOS; Charge density

## ABSTRACT

Spring back is a problem as important as tearing or thinning, while forming high-strength sheets. Spring back is an undesirable situation and it is the form difference between the desired form of a part in theory and the form obtained due to mechanical characteristics and process inputs of the material after die forming. It affects operations in shearing, punching or bending dies in subsequent operations in forming die sets. If the part is not within the desired tolerance range, it creates problems during assembly. In order for cost effective production plans for automotive parts to be made, suitable sheet forming simulations are needed. Waste of time and failures during die construction are minimized by defining accurate parameters by finite element analyses and minimizing periods of trial-and-error. In this study, the material SCGA1180DUB in sheet thickness of 1.2 mm from multi-phase steel sheet group was U-channelled, using Autoform sheet forming analysis program, according to appropriate process conditions having wall angles of 7°, 10°, 12° and die radius values of R3, R5, R8 and the spring back values were estimated. Mechanical properties of SCGA1180DUB high strength sheet were determined by tensile tests. The results obtained were compared through the finite element program and suitable wall angle and die radius values for the material SCGA1180DUB for forming advanced high-strength sheets were determined. As the die radii increased at the same wall angles, the amount of spring back increased significantly. In particular, due to high yield and tensile strength of multi-phase high strength sheet, spring back values were observed to be high. Negative spring backs were observed in the roof of the part. In the same die radii, under the same process conditions, as wall angles increase, spring back values decreased. In the literature, it is interesting that there are few studies regarding forming, spring back of high-strength sheets SCGA1180DUB. This study will contribute to the literature. Auto form program was used for Finite Element Analysis (FEA).

## INTRODUCTION

Sheet metal parts have been widely used for many years in many sectors such as aircrafts, vessels, automotive, major appliances. The main reasons for the widespread use of sheet metal parts can be listed as follows: Easy availability of raw materials, compatibility to machining, affordability, weldability, machineability of complex

geometries and formability. Particularly, springback is a problem as important as tearing or thinning, while forming high-strength sheets. Thinning causes the part to fail to show the performance that it needs to show as strength. The occurrence of wrinkling will cause appearance distortions in the part to be obtained after die forming process and surface deformation in die components. Springback is an undesirable situation and it is the form difference between the desired form of a part in theory and the form obtained due to mechanical characteristics and process inputs of the material after die forming. It affects operations in shearing, punching or bending dies in subsequent operations in forming die sets. If the part is not within the desired tolerance range, it creates problems during assembly. Young modulus, material type, yield and tensile strength, anisotropy coefficient ( $r$  value (0,45,90)), strain-hardening exponent ( $n$  value), forming speed, friction coefficient, surface roughness, thickness etc. are primary factors affecting sheet metal forming.

In their study, Şen, et al. performed Finite Element Analysis (FEA) to determine the proper bend radius ( $R$ ) depending on the sheet thicknesses ( $T$ ) in order to compensate the springback that occurs after U-type, L-type and Hood type DP600 sheet parts in different thicknesses and bend radii are formed. Die components drawn using CAD programs were introduced to simulation program. As a result of the analyses, it was observed that as the bend radius of the part in the same sheet thickness increases, the springback increases too; as the bend radius decreases, thinning increases and as the sheet thickness increases, springback values decrease [1].

Silva et al. noted that advanced high-strength sheets are widely used in automotive sector, particularly in body-in-white, it is of great importance to act in accordance with different and specific mechanical behaviors of dual-phase steels, compared to conventional steels, during die-forming. The researchers aimed to relate edge crack defect to local formability analysis, mechanical characteristics of the material and whole expansion ratio. Hole expansion ratios of DP steels were examined by finite element analysis during die forming, in order to avoid unexpected defects through finite element analysis [2].

Tisza and Czinege stated that automotive industry plays a decisive role in the economy of developed countries and mentioned the importance of applying lightweight construction of vehicles, meeting the demands of customers and the increasing legal requirements. Applying high strength materials is considered one of the most promising possibilities in order to meet these expectations. High-strength thin sheets contribute significantly to mass reduction. It has been seen that aluminum alloys, for instance, AA7021 and AA7075 have been used recently, besides high-strength steels such as DP1000, TRIP780. This study emphasizes aluminum alloys in regard to use of both new generation high strength steels and lightweight steels as to recent material developments in automotive industry. A comparison between steel and aluminum applications was made and various perspectives were brought to automotive industry [3].

Gomes, et al. stated that use of both high strength and lightweight materials; especially use of dual-phase steels stands out due to the requirements such as safety, comfort, vehicle weight reduction etc. However, characteristics of these steels and hybrid sheet metal process depend on springback. In their study, they aimed to minimize deviations and predict forming through simulations. They simulated a mathematical model and observed springbacks. Through tool nose compensations, they significantly reduced tool nose preparation costs and waste of time [4].

Radonjic and Liewald stated that high strength sheets provide advantages in vehicle manufacturing, when issues such as total weight reduction, passenger safety are taken into account. However, springback is the biggest problem in sheet metal forming. They noted that the use of small tool nose radii in initial simulations reduced springback. The same parameters were applied to the experimental setup in order to confirm the simulation results. Change in die radius had a different effect on cross-sections of the part. Optimization of the sheet had an effect on spring back [5].

Hattalli and Srivatsa stated that sheet metal industry has shown more technological advances since the last century and informed about sheet forming parameters. The transition from hand forming to finite element-based processes is technologically necessary. Reducing waste of time, trial-and-errors, processing costs, are important parameters. Sheet metals are formed by operations that include operations of bending, deep drawing, shearing and punching. As process parameters, punch radius, sheet temperature, blank holder force, tool nose measurements, sheet thickness are important. They noted that there are many studies in the literature about the defects of formed parts. Undesirable errors such as tearing, wrinkling and spring back are analyzed by experimental and simulation techniques [6].

Sulaiman, et al. analyzed springback in sheet metal forming process in different parameters using numerical method through ABAQUS program. Sheet thickness and sheet material were determined as different parameters in simulations. Analyzing springbacks of AISI 15B48H steel and carbon fiber reinforced composite material, they found that springback in composites is less compared to steels and noted that computer-aided simulations would cause decrease in physical tests required [7].

Sigvant, et al. stated that achieving effective results in forming process of sheet metal parts depends on tribological conditions, friction conditions and surface roughness. They stated that these friction conditions, surface roughness of coating and tools, lubricating and process conditions are important, but even though friction has a key importance, it is not considered in detail in sheet forming simulations. The authors introduced this model by developing a new friction model in their study. They created a simulation with different coatings and die elements of different hardness. Uneven tool surface roughness might require erroneous testing or additional testing during part manufacturing testing. Coatings such as zinc magnesium can reduce tool costs, affect the gliding speed and tool surface roughness [8].

Tang, et al. stated that they observed serious springback during forming of advanced high-strength sheets. Nonlinear characteristics of springback and expensive computational costs might constitute an obstacle for finite element analysis-based springback prediction. Researchers developed a projection-based heuristic global search method (P-HGS), to minimize springback due to nonlinear characteristics and expensive costs of springback. Blank holder forces were optimized and springback is reduced by this method. The recommended method can be used to predict springback in U-channel parts. Design variables were selected as blank holder in tri-phase and two critical times. Different drawbead designs were tried [9].

Pilthammar, et al. stated that sheet forming simulations are useful for solving forming problems. They stated that deformations of die and frictions in press line are generally disregarded. The aim of this study is to combine results of two different SE model and to develop a method to include die and press deformations of SMF simulations. They developed two SE models, two-dimensional (2S) hard tool surfaces and a SMF model, which is a structural model of die and press. This model can visualize relatively large and unexpected deformations of the die structure. This model can be used in testing dies, design of new dies or analysis of operating dies [10].

In their study conducted on finite element analysis, springback and compensation, Aslan and Karaağaç found that increase in ironing period decreases springback; that amounts of springback of materials are high due to high tensile of the materials during the forming process of sheet materials; that as bend angle increases, the amount of springback increases too; that decrease in bend radius reduces springback; that increase in yield strength and strain-hardening increases springback; that as temperature rises springback reduces while forming high-strength steels [11].

Esener, et al. aimed to reduce springback of the material SP600 of 0.8 mm thickness by performing parameter sensitivity analyses through experimental design. DYNAFORM software was used for Finite Element Analyses. Experimental design was made by selecting parameters of element formulation, number of integration points, blank holder force and friction coefficients. Simulations performed with the new parameters obtained, showed that springback reduced [12].

In their study, Çavuşoğlu and Gürün conducted uniaxial tensile tests at different deformation speeds to examine effects of deformation speed in deep drawing process of sheet materials DP600 and DP780 and determined mechanical characteristics of the materials. They performed deep drawing analyses at different deformation speeds of sheet materials using finite elements method. In conclusion of the study;

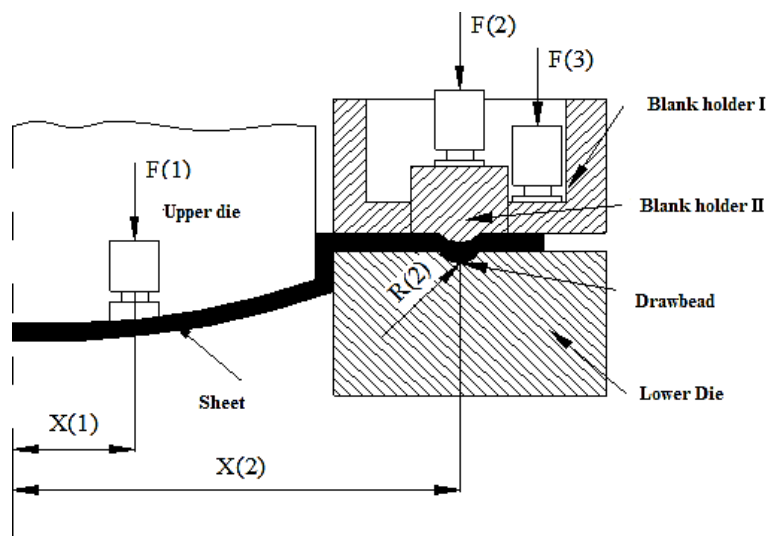
- As deformation speed increased, yield strength, tensile strength and percentage elongation of both materials increased.
- The sheet material DP780 was observed to have more spring back compared to the sheet material DP600 after the forming process.
- Since the sheet material DP780 has a higher strength than the sheet material DP600, more die force is needed.
- It was observed that as the deformation speed increased, thickening occurred in bottoms of the parts [13].

Suttner, et al. stated that lightweight materials such as magnesium alloys can be used instead of conventional sheet materials due to the welding saving, light design and dimensional accuracies and they emphasized that deep drawing process will occur at high temperatures due to hexagonal lattice structures of magnesium alloys. They stated that springback of magnesium alloys should be analyzed due to its mechanical characteristics during deep drawing process at high temperatures and they examined the spring back behavior at 0 and 90 rolling directions in their study [14].

### Literature review

Kayabaşı examined three approaches to minimize springback, wrinkling and thickness errors. Dual blank holder was used in the first approach (Figure 1). In the second approach, optimum forming parameters were determined by optimization method depending on the parameters. Finite element analysis, response surface methodology and genetic algorithm were used in combination to find suitable values. In the third approach, a probability was developed to predict die failures. As a result of optimization process performed by genetic algorithm, it was observed that the values of springback, wrinkling and thickness reduction significantly decreased. It was understood from the optimization results that when optimization criteria change, the process parameters  $X(2)$ ,  $R(R)$  and  $F(1)$  did not change and  $F(3)$  changed very little. In conclusion of the study, the author stated that optimization methodology can be successfully used in forming processes in automotive industry [15].

Figure 1. Forming parameters.



Peixinho, et al. examined the forming by adding rings of different hardness to blank holder by creating an experimental and numerical setup to increase forming limits of high-strength sheets. In their study, they aimed to reduce deformations in blank holder while forming high strength sheets. Besides, they noted that complex parts can be formed in fewer steps by adding rings of different hardness to blank holder through cold forming without hot forming [16].

Houa, et al. stated that clearer results were obtained when the mechanical tests of the material were conducted based on the results obtained, in order to obtain springback prediction through finite element analysis. In this study, the yield strength behaviour model of MP980 sheet steel was applied and compared according to yield criteria Hill48, Barlat89, Barlat2000. They stated that they obtained accurate springback predictions using suitable yield criteria by performing finite element analyses of U-channel parts in different tool nose radii ( $R6$ ,  $R8$ ,  $R12$ ) on LS-DYNA program [17].

Tisca, et al. stated that high-strength steels continue to develop in line with demands in the automotive industry such as less fuel consumption, comfort, less harmful emissions, safety and better performance. In particular, dual-phase steels continue to develop. However, there are always problems in forming high-strength sheets. Authors prepared a new experiment method, examined mechanical characteristics of dual-phase steels DP600, DP800, DP1000 and stated that  $\gamma$  and K parameters are of great importance for simulation in springback behaviour of dual-phase high strength sheets. They conducted various numerical simulations by reflecting different  $\gamma$ , K, E values to see how springback behaviour of the tested material changes (Table 1) [18].

**Table 1.** Mechanical characteristics of dual-phase steel sheets.

	DP600				DP800				DP1000			
	I.	II.	III.	IV.	I.	II.	III.	IV.	I.	II.	III.	IV.
$\gamma$	0.22	0.177	0.154	0.123	0.22	0.161	0.131	0.113	0.2	0.146	0.117	0.094
X	49	45	30	37	82	65	54	46	80	68	60	57
E, GPa	160	170	174	180	160	173	179	183	165	176	182	187

Galdos, et al. examined the steel Fortiform 1050, one of the third generation steels, under die conditions numerically and experimentally and predicted final springback values. The authors demonstrated the importance of friction coefficient, elastic modulus and deformation hardening in their springback predictions. Similar contact behaviors observed in DP steels, were observed with the new tribological study [19].

Radonjic and Liewald noted that high-strength sheets provide superior properties for passenger safety and weight reduction, but stated that springback during forming is a serious problem. They examined the springback values of the sheet with U-channel material DP980 in different tool nose radii. They noted that the amount of springback reduced in smaller tool steels. When the blank holder force increased from 300 Kn to 1500 Kn, the wall angle change, sidewall curl and sheet edge bending decreased in experiments. The results were confirmed by simulations. When the blank holder force increased from 300 kN to 1500 kN, the wall angle change, sidewall curl and sheet edge bending decreased by 20%. While simulations confirmed wall angle results by YU model, they did not confirm sidewall curl. The Hill 48 model did not give experiments results. In simulations, it was observed that wall angle deviations decreased by 10% with maximum blank holder force. Compared to simulations with original 202 GPa elastic modulus, larger springbacks were observed with a small elastic modulus of 140 GPa and with BHF force of 300 kN, whereas less springbacks were observed with BHF of 1500 kN [20].

Esener and Gürsoy performed analyses with four different material models: isotropic material-admitting isotropic strain-hardening (power law), anisotropic material-admitting isotropic strain-hardening Hill-48, Barlat-89 and anisotropic material-admitting kinematic strain-hardening; by modelling deep drawing, square box drawing and V-bending dies with materials DP600, DP980, DC05 and AA5754 in order to measure sensitivities of material models in finite element analyses. As a result of the analyses conducted, more appropriate results were obtained with the kinematic strain-hardening material model, compared to other material models and it was seen that more parameters are needed in kinematic strain-hardening material model [21].

Karabulut, et al. aimed to demonstrate usability of thinner sheets and advanced high-strength sheets that are stronger and better formable compared fo 1st generation steels and cheaper compared to 2nd generation steels, in vehicles instead of current sheets that are being used for vehicle weight reduction. Pole A, Pole B and Pole C were re-designed using 3rd generation TBF steel by autoform program, critical radius values, wall angles were revised and productibility limits were evaluated (Figures 2 and 3). They offered suggestions for critical cross-sections of parts (Figures 4 and 5) They noted that mechanical characteristics of 3rd generation TBF steel is suitable for die; that there should be big radii instead of gradual transitions in part design and that no cross-section should be left in negative angle [22].

**Figure 2.** Single-piece A and B pole part, for which simulation study was performed.

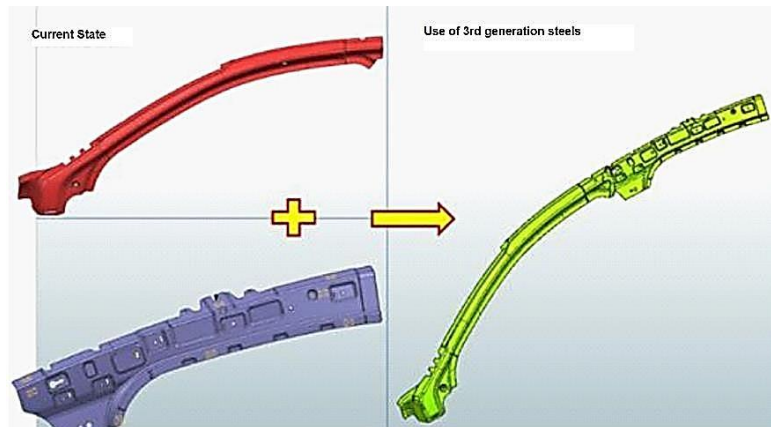


**Figure 3.** Single-piece A and B pole part, for which simulation study was performed [22].

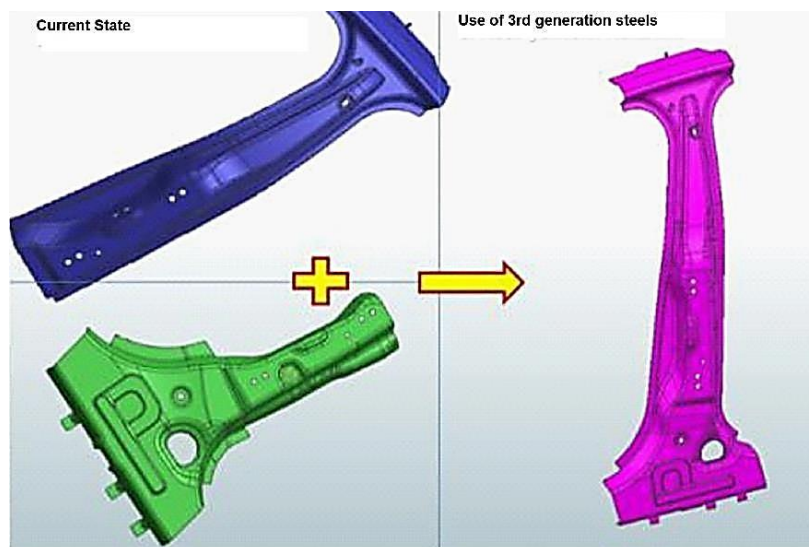


Figure 4 shows that sheet qualities have different strengths and elongations. Various negative situations arise, while strength increases in sheet grades. There are situations where sheet grades are advantageous and disadvantageous compared to each other. Springback values should be taken into consideration while evaluating the design compatibility of parts. The compatibility of the part for cold forming or hot forming is an important point to be determined. Designers have many sheet alternatives. Besides, simulation programs continue to develop. Along with the process design, defects on drawing surfaces are minimized by simulation programs and die trial periods are minimized during die manufacturing.

Figure 4. Elongation and break values of steel grades.

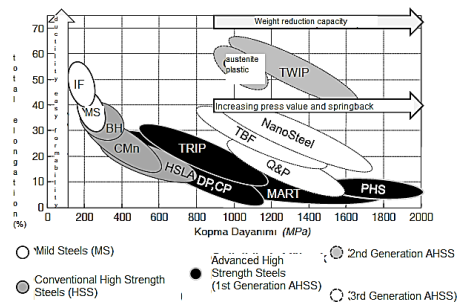
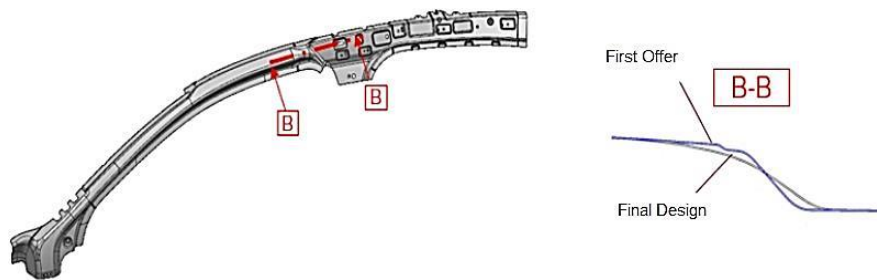


Figure 5. Improvement work in the B-B cross-section in the a pole part.



Esener conducted sheet forming performance analysis of the material DP600 using Yoshida-Uemori plasticity model, Hill 48 plasticity model and Power law plasticity model using Ls-Dyna software. Comparing the experiment results with results of finite element analysis, it was found that prediction performance of Power Law plasticity model was low, kinematic strain-hardening models are effective in forming sheet metal dies [23].

Karaağaç and Aydın experimentally performed V-bending to observe the springbacks of the sheet materials DP600 and HSLA300 in different die angles and different ironing periods. In conclusion of the experiments, springback of DP600 sheet material was found to be 12% higher than that of HSLA300. It was seen that as ironing period increases, springback decreases. With the increase of the die angle, springback angle of both materials increased, then decreased [24].

Tuyan and Demirer discussed the tearing problem that occurs during die-process of wishbone part used in vehicles and offered various solutions. In the study, finite element analyses were performed by Autoform software using sheets DD13 and S355MC. When parts obtained from the die were compared, there was tearing in areas considered risky (Figure 6). Geometry change was applied for torn areas, teflon with 0.25 mm thickness and heat treatment were applied to reduce friction and polishing in risky areas. The researchers offered solutions to solve the problem in the part without increasing the number of operations. Die-cast parts were subject to fatigue test and it was detected that there was no tearing in the parts [25].

Figure 6. Tearing values.

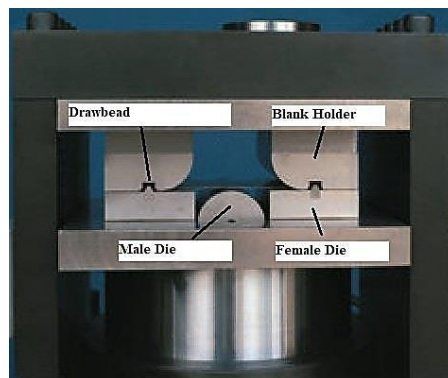


The steels DP450 and DP800 were subjected to tensile tests in 4 different deformation speeds, 3 different rolling directions (0, 45, 90) and mechanical characteristics of the materials were examined. In conclusion of the study, deformation speed increased while elongation values decreased. Deformation speed as an obvious effect on the material DP450, besides attention should be paid for the part not to be deformed during cold forming. Higher strength values were observed in both materials in the 45° rolling direction. It was found that the deformation speed had greater effect on strength values than rolling direction [26].

Billur, et al. performed finite element analysis and experimental analysis to predict spring backs after bending, by performing V-bending in two different course profiles of the steels TWIP 980, TBF 1050 and Q&P 1180 provided through servo press. As a result of the analyses, the steel TWIP 980 was found to provide superior formability. Simulation and experiment results were found to be compatible in the steels TWIP 980, TBF 1050. Compared to other steels, the steel Q&P showed higher spring back. It was evaluated that there might be residual austenite in the advanced high strength steels studied and that the elastic modulus might not be constant due to plastic strain. Additionally, since phase changes will not be homogeneous, the mechanical characteristics of the part might not be the same in every area of the part [27].

Drawbeads are used as a control mechanism in sheet metal dies, to control flow of sheet material into die cavity (Figure 7). Therefore, flow control is an important parameter in sheet metal forming. Problems such as spring back, wrinkling, tearing, thinning that occur during sheet metal forming processes are eliminated through control of the sheet. İriç, et al. examined the change of restraining force depending on the draw bead height and developed a mathematical model using the results obtained. Mathematical results and results of finite element analysis were found to be compatible [28].

**Figure 7.** Location of draw beads in the die.



Özdemir, et al. examined the formability analyses of the steel sheets HX220YD, DX54D, DX52D, S500MC, HCT600X, HX340LAD using finite elements method. Materials having 1.6 mm sheet thickness were analyzed using Autoform software. In conclusion of the analyses, formabilities of the parts were interpreted through formability limit diagrams. Due to their effect of reducing the average grain size in steels, Niobium, Titanium, Vanadium, Carbon, Manganese and Copper were observed to increase the yield and tensile strength of materials, but negatively affect their formability. Aluminum, on the other hand, had a positive effect on forming [29].

Due to reasons such as die tool life, product form, flow of the sheet into the die, friction is an important parameter in sheet metal forming. Mechanical characteristics, friction conditions, contact values of the material are important especially for the accuracy of the results of finite element analysis. Kalkan, et al. developed a new method of determining the friction coefficients to determine friction coefficients in radial shrinkage area and stretching area. In the stretching area, as depth of deep drawing increased, the friction coefficient, although slightly, decreased, use of paraffin as a lubricant caused the friction coefficient to decrease. Graphite lubricant reduced the friction coefficient in radial shrinkage area [30].

Kılıç and Öztürk experimentally examined the forming and spring back values of the steel TWIP900 and compared its flow surfaces and formability limit diagrams with the steel DP600, which is commonly used in the market. By performing bending process in V-die it was seen that more spring backs occurred in the steel TWIP900 than in the steel DP600. Simulation material models must be defined accurately, limit forming values must be defined completely in order to minimize periods of trial-and-error in the dies. According to the results obtained, it was found that the steel TWIP900 will greatly contribute to weight reduction, that its high formability ratio and energy damping will provide a great advantage, however spring back is a big problem. It was assessed that it would be appropriate to use the Swift model for the TWIP steel analysis on finite element programs [31].

Taşdemir analyzed the effects of different die geometry on deep drawing process by finite element method using 4 different die geometries: flat, curved, elliptical and 45 degrees slope. Female die forms were found to be critically important for control of flow of sheet into the die in sheet forming. In the flat form, it was seen that the sheet was torn, the acceptable values were obtained in R6 die structure [32].

The sheet material  $^{46}\text{Mo}_3$  was normalized without heat treatment, tempered (13 and 30 min.) and then V-bent in 3 different types; its spring-forward and spring-back values were examined. In conclusion of the experiments, it was found that keeping the sheet for 30 minutes waiting, after it is formed by punch, reduces spring forward and spring back. As the punch stays on the sheet for a long time, the stretching in the internal structure of the material decreases. It was found that spring-forward occurs in normalization process without heat treatment, and spring-back occurs in tempering process [33].

In this study, finite element analysis of the multi-phase high strength sheet SCGA1180DUB was performed using Autoform analysis program, 3 different wall angles and spring back values at 3 different die angles of the U-channel part were measured and compared. Finite element analysis is a method used in feasibility studies of automobile parts. Feasibility studies are completed before starting die manufacturing. The final design is decided according to the desired forming criteria, thinning values, and spring back values. At this point, defining the appropriate process values such as wall angles and die radii into the analysis program will minimize waste of time. In the literature, it is interesting that there are few studies regarding forming and spring back of multi-phase high-strength sheets SCGA1180DUB. This study will contribute to researchers.

## MATERIALS AND METHODS

Neodymium In our study, U-bending die design of the material SCGA1180DUB with a thickness of 08 mm was performed and its springback behavior at wall angles  $7^\circ$ ,  $10^\circ$  and  $12^\circ$  and die radii R3, R5, R8 was examined. Tables and graphs obtained by finite element method were compared. Springback is an important problem for advanced high strength sheets. Compensating this problem in feasibility studies is very important. The finite element analysis method is widely used in all engineering applications. Experimental studies increase periods of trial-and-error, resulting in waste of time, material and money [11].

For the experimental research, 1.2 mm thick SCGA1180DUB high strength steel used in the automotive industry was chosen. It was subjected to tensile tests in 3 rolling directions to define the mechanical properties of the material in the  $0^\circ$ ,  $45^\circ$  and  $90^\circ$  rolling directions. Tensile tests (Table 2).

**Table 2.** Mechanical characteristics of SCGADUB1180.

Hadde yönü	Rp0.2 (MPa)	Rm (MPa)	$\delta$ (%)	r değeri
$0^\circ$	904.84	1217.74	6,34	6,34
$45^\circ$	911.55	1202.01	4,88	4,88
$90^\circ$	909.71	1221.23	5,73	5,73

Today, high strength sheets continue to be developed in space, major appliances and particularly automotive sectors due to vehicle weight reduction, vehicle safety, vehicle cost reduction and environmental factors. Particularly, high strength sheets are used in areas of the vehicle that require strength against collision, such as door bars, columns, bumper beams, seat rails, side beams. Özcan, et al. examined the micro structures of the high strength steels 590 DU, 980 DUB, 1180 DUB, determined their mechanical characteristics and applied resistance spot welding. They aimed to optimize the welding parameters using Taguchi method. When micro structures were examined, 81.8% ferrite, 18.2% martensite were found in the material 1180 DU; and 85.7% ferrite, 14.3%

martensite in 590 DU. It was seen that martensite ratio is higher in high strength sheets. In dual-phase sheets, ferrite provides elongation and martensite provides strength (Tables 3 and 4)<sup>[34]</sup>.

**Table 3.** Mechanical characteristics of sheets.

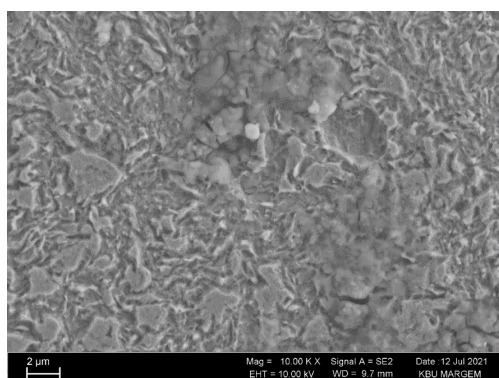
Steel	Yield strength (Rp0,2) (MPa)	Tensile strength (Rm) (MPa)	Elongation (A) (%)
590 DU	366	629	28.3
980 DUB	669	1058	14.3
1180 DUB	840	1212	9.3

**Table 4.** Chemical structure of sheets.

□Steel	C	Si	Mn	P	S	Al	Ti	Nb	B
590 DU	0.083	0.236	1.87	0.016	0.0022	0.037	0.002	0.002	0.0004
980 DUB	0.155	0.194	2.29	0.01	0.0004	0.055	0.003	0.024	0.0003
1180 DUB	0.166	0.378	2.49	0.007	0.0005	0.052	0.033	0.002	0.0024

The internal structure of DUB1180 high strength steels is shown in Figure 8a. The samples, which were mounted for microstructure examination, were first sanded. Afterwards, the samples were polished. The polished samples were prepared for etching by applying alcohol on their surfaces. Microstructure photographs of the materials whose surfaces were cleaned after etching were taken. As a result of the analysis, it is seen that the white islands are martensite and the gray parts are ferrite (Figure 8). The hardness value was measured at 37-38 HRC in the measurement made on the Rotwel surface hardness measuring device.

**Figure 8.** (a) Internal structures (b) Post-test tensile test specimens.



a.



b.

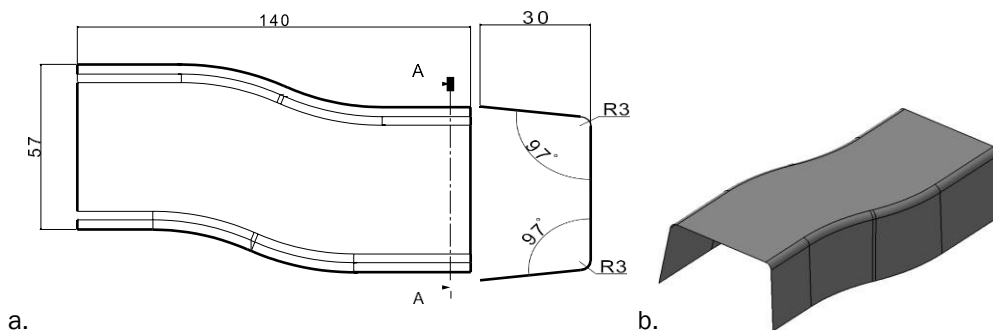
Steel producers are developing weldable steels with high strength, high formability with the statutory obligations in the automotive industry, vehicle weight reduction, high strength vehicle requests. We can say that 3rd generation high strength steels will have a wide range of use in the future due to their weldability properties and high strength feature, and their lower costs compared to the 1st generation high strength steels. Standard tension test of the high strength steels may not be enough for simulation research as well. Detailed tests should be conducted for the simulation results to be accurate <sup>[35]</sup>.

Murathan and Kılıçlı stated in the detailed literature research regarding nano bainitic steels giving the information about the bainite internal structure, mechanical properties, chemical composition, transformation mechanism, that nano bainitic steels with mechanical properties could be produced without the need for very expensive alloys and mechanical processes. Nano bainitic steels show good toughness and high tensile strength but their non-weldability as a result of containing high carbon is considered as disadvantageous <sup>[36]</sup>.

### Design of die and part

In order to see springback and formability values the part in Figure 9 is designed in Catia V5 software. The tensile depth of the part is 30 mm. Springback on the side walls and on the top will be examined. The part will be measured in 60 mm cross-sections from the center, right and left of the part.

Figure 9. (a) Cad Model of the Part (b) The Formed Part.



Mechanical properties loaded in autoform software is shown in Table 5. Die components are shown in Figure 10. The sheet is formed by squeezing it between the blank holder and the female die and it is formed by perfusing on the male die.

Figure 10. Die components.

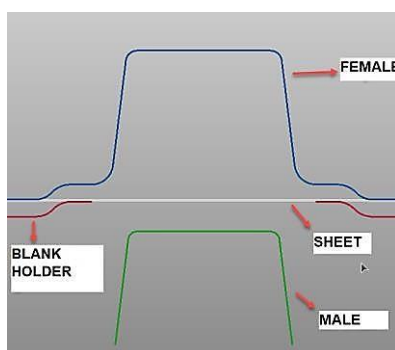


Table 5. Mechanic properties of the materials defined to autoform program.

Elastic modulus (MPa)	2.10E+05
Poisson's Ratio Density (kg/m <sup>3</sup> )	0.3
Yield strength (MPa)	909.71
Tensile Strength (MPa)	1221
Strain-hardening exponent	0.119
ro	0.78
r45	0.76
r90	0.78
Volumetric Heat Capacity (mJ/(mm <sup>3</sup> K))	3.64
Density (MPa/mm)	7.90E-05
Elongation (A) (%)	8.32

### Experimental studies

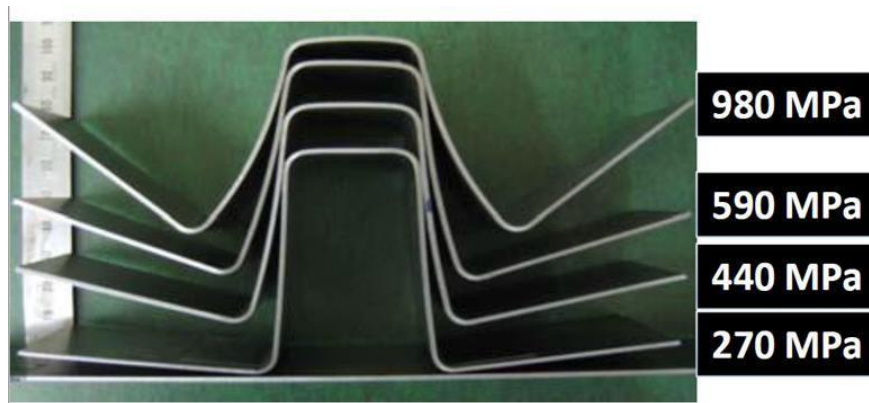
Finite element analysis is a technique that examines the behaviour of a part under applied forces and pressure, and renders information about situations about a real object under applied loads. Part behaviour could be expected and debugged with the assistance of finite element analysis [37]. Jadhav, et al. stated that since the traditional production planning method takes too much time, the Finite Element Method (FEM) is conducted to reduce production time. The Finite Element Method (FEM) builds upon the selection of the appropriate material model, the accuracy of the input parameters, actual operation values, and other situations. In this research, we aimed at validating new developments on sheet forming, parameters affecting sheet forming, and these parameters. In the first research, the springback of AlMgSi panel part was examined, springback on the aluminum panel was calculated more than once and compensated successfully. In the second research, deformation and thickness change in the process of hot forming were examined [38].

Esener, et al. simulated die set of the 0.8 mm DP600 roof support sheet which is an industrial product, with Autoform software. According to the first results obtained, compensated surfaces were created and re-simulated. It was observed that the die compensation was effective in reducing the springback [39].

Sayin and Basmacı examined springbacks of the copper sheets in V-bending dies, different thickness, different die angle and different bending radii experimentally. In the experiment results, it was observed that as the die bending radius increased, the springback decreased, as the thickness of the sheet plate increased, the springback decreased, and the springback values obtained from 2 mm radius dies were less than 4 mm radius dies [40].

As the strength values of the sheets increase, the forming difficulties arise. As the strength of the material increases, the springback values decrease (Figure 11) [41].

**Figure 11.** Springback values for materials with various strength values [41].



Experimental variable parameters in the research are given in Table 6.

**Table 6.** Experimental parameters and parameter values.

Experimental parameters	Parameter values
Material	SCGA1180DUB
Wall Angle	7°,10°,12°
Die Radius	R3, R5, R8

Springback value will be measured at 7°,10°,12° wall angles and R3, R5, R8 die radii, the 3 cross-sections specified in Figure 12 and at 9 points in each cross-section. Figure 13 shows the cross-sections and points measured in autoform program.

Figure 12. Cross-sections and points to be measured.

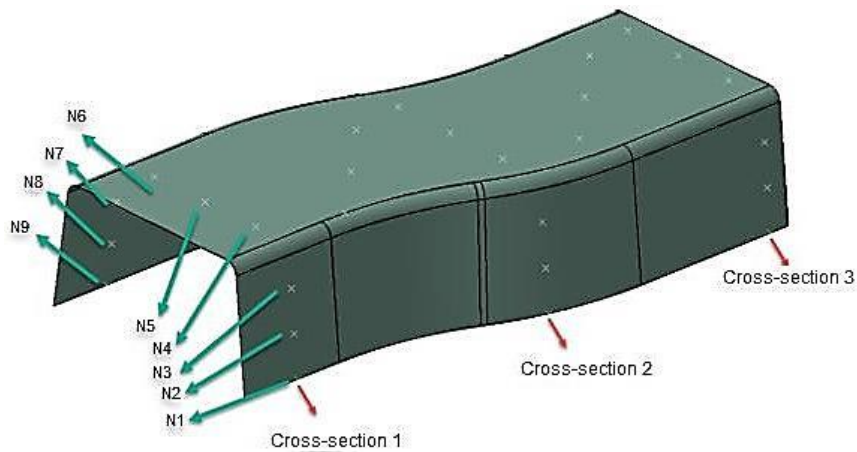
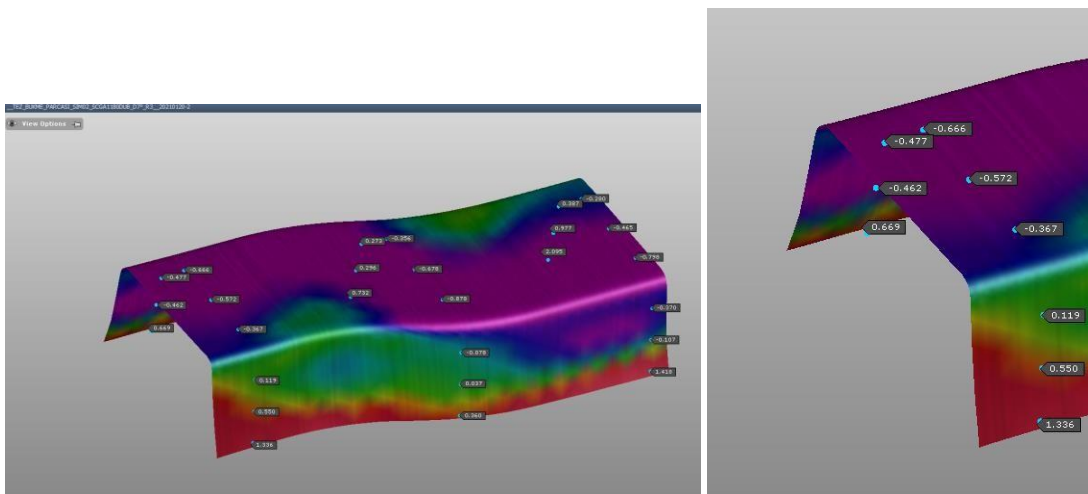


Figure 13. Cross-sections and points measured in autoform program.



## RESULTS AND DISCUSSION

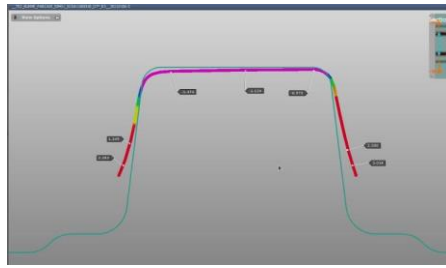
The springback behaviour of the part at wall angles  $7^\circ$ ,  $10^\circ$  and  $12^\circ$  and die radii R3, R5, R8 was examined. Springback values were obtained from 27 different measurement points in 1 part, including 9 points in 3 cross-sections (Table 7).

Red colored area in Figures 13 and 14 shows the part springs back positively, pink colored area shows springback in a negative way, green areas show the springback is acceptable.

Table 7. Shows springback values measured.

Wall Angle	Points	Die Radius:3 mm			Die Radius:5 mm			Die Radius:8 mm		
		R:3 Cross-Section:1	R:3 Cross-Section: 2	R:3 Cross-Section: 3	R:5 Cross-Section: 1	R:5 Cross-Section: 2	R:5 Cross-Section: 3	R:8 Cross-Section: 1	R:8 Cross-Section: 2	R:8 Cross-Section: 3
°	N:1	1.336	0.36	1.418	2.47	2.054	2.738	2.874	3.04	3.258
	N:2	0.55	0.037	-0.107	1.289	1.031	0.548	1.626	1.551	1.365
	N:3	0.119	-0.078	-0.37	0.628	0.445	0.017	0.914	0.59	-0.076
	N:4	-0.367	-0.878	-0.798	-0.855	-1.116	-1.434	-1.395	-1.545	-2.237
	N:5	-0.572	-0.678	-0.465	-1.184	-1.228	-1.176	-1.814	-1.775	-1.895
	N:6	-0.666	-0.356	-0.28	-1.513	-1.186	-1.025	-2.205	-1.694	-1.794
	N:7	-0.477	0.273	0.387	-0.259	0.34	0.667	-0.18	0.503	1.128
	N:8	-0.462	0.296	0.977	0.221	0.876	1.605	0.938	1.245	2.229
	N:9	0.669	0.732	2.095	1.75	1.725	3.018	2.936	2.557	3.425
10°	N:1	1.375	0.463	0.895	2.414	1.481	2.736	2.468	2.339	3.452
	N:2	0.374	0.002	-0.199	1.224	0.761	0.815	1.484	1.228	1.362
	N:3	0.157	-0.003	-0.14	0.467	0.239	0.06	0.68	0.435	-0.192
	N:4	-0.367	-0.819	-0.709	-0.805	-1.236	-1.478	-1.34	-1.596	-2.174
	N:5	-0.674	-0.769	-0.552	-1.197	-1.275	-1.17	-1.768	-1.786	-1.829
	N:6	-0.811	-0.632	-0.365	-1.52	-1.217	-0.991	-2.179	-1.707	-1.702
	N:7	-0.245	-0.218	0.299	-0.147	0.405	0.63	-0.167	0.258	0.481
	N:8	-0.434	-0.236	0.969	0.224	0.696	1.038	0.521	1.08	1.516
	N:9	0.273	0.606	1.585	1.637	1.423	2.117	1.465	2.077	3.033
12°	N:1	0.871	0.31	0.822	1.827	1.013	1.527	2.067	1.972	2.601
	N:2	0.221	0.01	-0.179	0.61	0.441	0.435	0.958	0.951	0.841
	N:3	-0.053	-0.134	-0.125	0.289	-0.122	0.06	0.392	-0.058	-0.407
	N:4	-0.393	-0.913	-0.672	-0.916	-1.345	-1.443	-1.46	-1.766	-2.181
	N:5	-0.584	-0.766	-0.51	-1.188	-1.359	-1.12	-1.691	-1.874	-1.801
	N:6	-0.653	-0.589	-0.394	-1.431	-1.254	-0.963	-1.974	-1.675	-1.615
	N:7	-0.167	0.271	-0.018	-0.061	0.247	0.384	-0.408	0.231	0.664
	N:8	-0.497	0.264	0.318	0.228	0.691	1.143	0.727	1.136	1.727
	N:9	0.052	0.492	1.19	1.223	1.43	2.107	1.948	1.99	3.095

Figure 14. Schematic demonstration of springback in 7° wall angle and R5 cross-section 1.



**Examination of springback according to die radii**

In Figure 15, in cross-section 1(a) graph, in which the wall angle was 7°, springback value increased by 115% when the die radius went from R3 to R8 at the first point. Springback values also increased at similar rates when the die radius increased from R3 to R8 at other points in cross-section 1. Negative springbacks were observed in the roof of the part at points N4, N5, N6. Spring back value increased by 280% when the die radius went from R3 to R8 at the N4 point. As could be observed from the graph, negative springbacks are allowable in the die, where the die radius is R3. As the die radius increases, negative springbacks increase.

In Figure 15, in cross-section 2 (b) graph, in which the wall angle was 7°, springback value increased by 744% when the die radius went from R3 to R8 at the first point. Spring back values also increased when the die radius increased from R3 to R8 at other points in Cross-Section 2. Negative springbacks were observed in the roof of the part at points N4, N5, N6. Springback value increased by 77% when the die radius went from R3 to R8 at the N4 point. As the die radius increases, negative springbacks increase.

In Figure 16, in cross-section 3(c) graph, in which the wall angle was 7°, springback value increased by 129% when the die radius went from R3 to R8 at the first point. Springback values also increased when the die radius increased from R3 to R8 at other points in Cross-Section 3. Negative springbacks were observed in the roof of the part at points N4, N5, N6. Spring back value increased by 182% when the die radius went from R3 to R8 at the N4 point. As the die radius increases, negative springbacks increase.

Figure 15. Wall angle 7° spring back values (a). cross-section 1 (b). cross-section 2

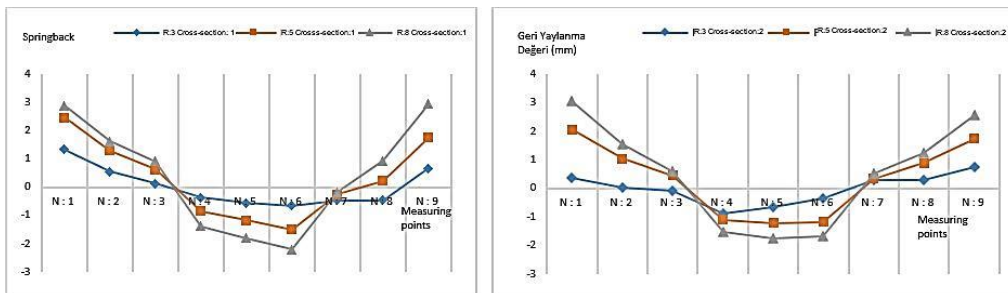
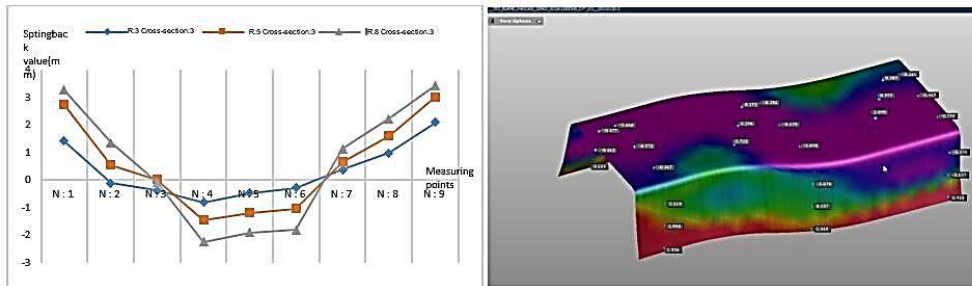


Figure 16. Wall angle 7° springback values (c). Cross-Section 3 (d) Wall angle 7° R3 springback values



In Figure 17, in cross-section 1 (a) graph, in which the wall angle was 10°, springback value increased by 79% when the die radius increased from R3 to R8 at the first point. Springback values also increased at similar rates when the die radius increased from R3 to R8 at other points in cross-section 1. Negative springbacks were observed in the roof of the part at points N4, N5, N6. Springback value increased by 267% when the die radius increased from R3 to R8 at the N4 point. As the die radius increases, negative springbacks increase.

In Figure 17, in Section 2 (b) graph, in which the wall angle was 10°, springback value increased by 403% when the die radius increased from R3 to R8 at the first point. Springback values also increased positively when the die radius increased from R3 to R8 at other points in Section 1. Negative springbacks were observed in the roof of the part at points N4, N5, N6. Springback value increased by 94% when the die radius increased from R3 to R8 at the N4 point. As the die radius increases, negative springbacks increase at the similar rate.

In Figure 18, in Section 3 graph, in which the wall angle was 10°, springback value increased by 285% when the die radius increased from R3 to R8 at the first point. Springback values also increased positively when the die radius increased from R3 to R8 at other points in Section 1. Negative springbacks were observed in the roof of the part at points N4, N5, N6. Springback value increased by 206% when the die radius increased from R3 to R8 at the N4 point. As the die radius increases, negative springbacks increase at the similar rate.

Figure 17. Wall angle 10° springback values (a). cross-section 1 (b). cross-section 2

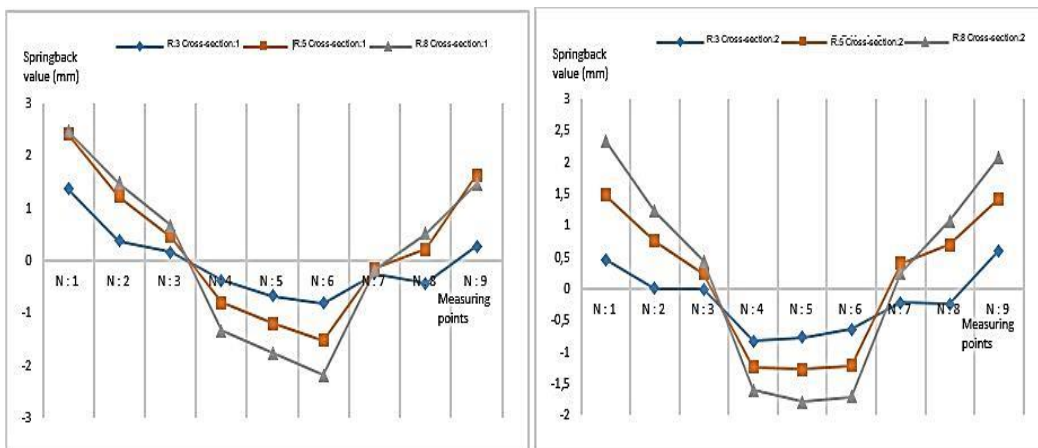
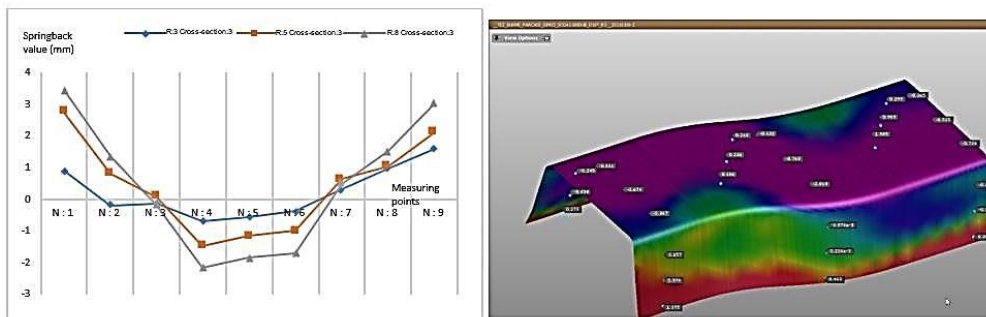


Figure 18. Wall angle 10° springback values (c). cross-section 3 (d) Wall angle 10° R3 springback values



In Figure 19, in cross-section 1 (a) graph, in which the wall angle was 12°, springback value increased by 136% when the die radius increased from R3 to R8 at the first point. Springback values also increased when the die radius increased from R3 to R8 at other points in cross-section 1. Negative springbacks were observed in the roof of the part at points N4, N5, N6. Springback value increased by 271% when the die radius increased from R3 to R8 at the N4 point. As the die radius increases, negative springbacks increase.

In Figure 19, in Cross-Section 2 (b) graph, in which the wall angle was 12°, springback value increased by 536% when the die radius increased from R3 to R8 at the first point. Springback values also increased when the die radius increased from R3 to R8 at other points in Cross-Section 1. Negative springbacks were observed in the roof of the part at points N4, N5, N6. Springback value increased by 93% when the die radius increased from R3 to R8 at the N4 point. As the die radius increases, negative springbacks increase.

In Figure 20, in Cross-Section 3 (c) graph, in which the wall angle was 12°, springback value increased by 216% when the die radius increased from R3 to R8 at the first point. Springback values also increased when the die radius increased from R3 to R8 at other points in cross-section 1. Negative springbacks were observed in the roof of the part at points N4, N5, N6. Springback value increased by 224% when the die radius increased from R3 to R8 at the N4 point. As the die radius increases, negative springbacks increase.

Figure 19. Wall angle 12° springback values (a) cross-section 1 (b) cross-section 2.

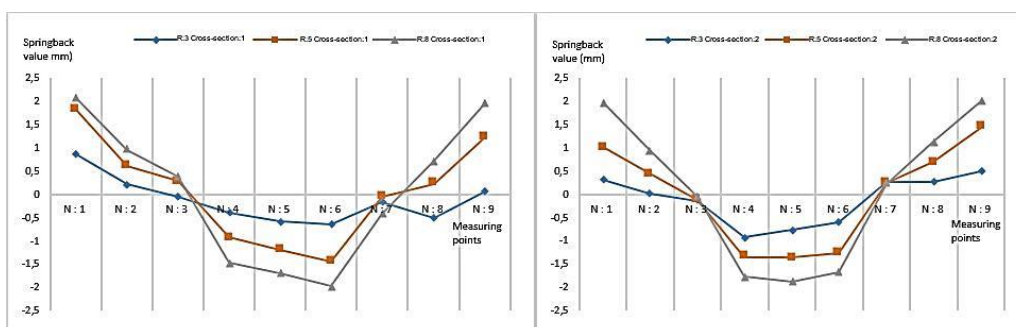
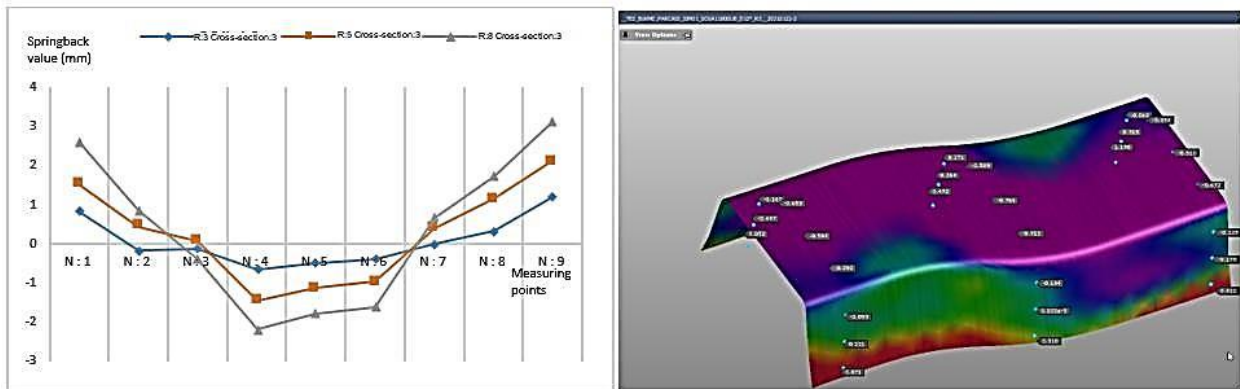


Figure 20. Wall angle 12° springback values (a). Cross-Section 3 (b) Wall angle 12° R3 springback values



**Examination of the springback in accordance with wall angles.**

According to Cross-Section 1 graph, the springback values in cross-section 1 in R3 die radius were examined. When the springback value in N1 was examined, it was found that the springback value decreased by 53,3% when the wall angle increased from 7° to 12°. The springback values in cross-section 1 also decreased with the increase of the wall angle at other points. Negative springbacks were observed at points N4, N5, N6, N7, N8. When the springback value in N9 was examined, it was found that the springback value decreased by 1186% when the wall angle increased from 7° to 12° Figure 21(a).

Figure 21(b) According to the Cross-Section 2 graph, the springback values in cross-section 2 in R3 die radius were examined. When the springback value in N1 was examined, it was found that the springback value decreased by 15% when the wall angle increased from 7° to 12°. The springback values in cross-section 2 also decreased with the increase of the wall angle at other points. Negative springbacks were observed at all wall angles at points N4, N5, N6. Negative springbacks were observed at points N4, N5 at the wall angle of 10°. When the springback value in N9 was examined, it was found that the springback value decreased by 48,7% when the wall angle increased from 7° to 12°.

Figure 22 according to the Cross-Section 3 graph, the springback values in cross-section 3 in R3 die radius were examined. When the springback value in N1 was examined, it was found that the springback value decreased by 72% when the wall angle increased from 7° to 12°. The springback values in cross-section 2 also decreased with the increase of the wall angle at other points. Negative springbacks were observed at all wall angles at points N4, N5, N6. Negative springbacks were observed at points N4, N5 at the wall angle of 10°. When the springback value in N9 is examined, it was found that the springback value decreased by 76% when the wall angle increased from 7° to 12°.

Figure 21. Die radius R3 springback values (a). Cross-Section 1 (b). Cross-Section 2.

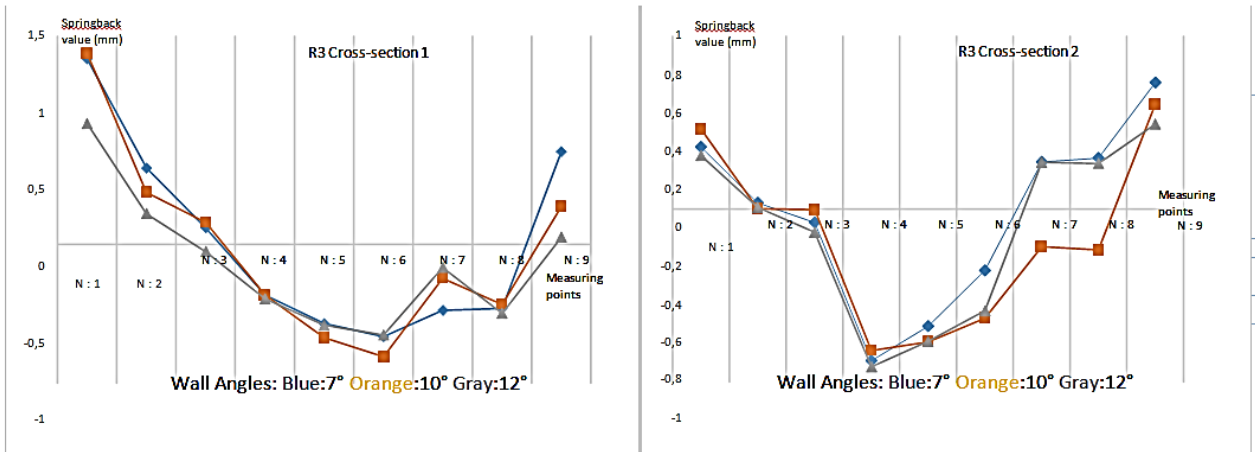
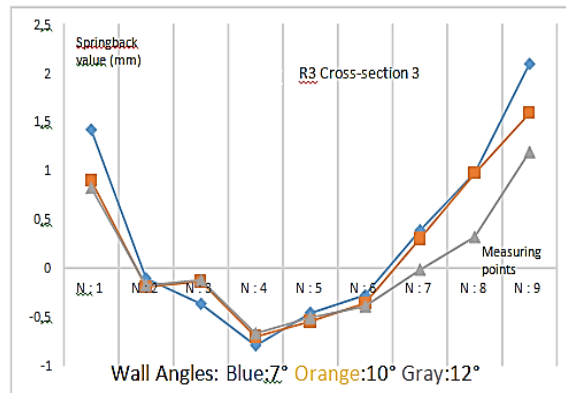


Figure 22. Die radius R3 springback values cross-section 3.



According to the cross-section 1 graph, the springback values in cross-section 1 in R5 die radius were examined. When the springback value in N1 was examined, it was found that the springback value decreased by 35% when the wall angle increased from 7° to 12°. The springback values in cross-section 1 also decreased with the increase of the wall angle at other points. Negative springbacks were observed at all wall angles at points N4, N5, N6, N7, springback values were nearly equal. When the springback value in N9 was examined, it was found that the springback value decreased by 43% when the wall angle increased from 7° to 12° Figure 23(a).

According to the cross-section 2 graph, the springback values in cross-section 2 in R5 die radius were examined. When the springback value in N1 was examined, it was found that the springback value decreased by 102,7% when the wall angle increased from 7° to 12°. The springback values in cross-section 2 also decreased with the increase of the wall angle at other points. Negative springbacks were observed at all wall angles at points N4, N5,

N6, springback values were nearly equal. When the springback value in N9 was examined, it was found that the springback value decreased by 20,6% when the wall angle increases from 7° to 12° Figure 23(b).

According to the cross-section 3 graph, the springback values in cross-section 3 in R5 die radius were examined. When the springback value in N1 was examined, it was found that the springback value decreased by 79% when the wall angle increased from 7° to 12°. The springback values in cross-section 3 also decreased with the increase of the wall angle at other points. Negative springbacks were observed at all wall angles at points N4, N5, N6, springback values were nearly equal. When the springback value in N9 was examined, it was found that the springback value decreased by 43,2% when the wall angle increased from 7° to 12° Figure 24.

Figure 23. Die radius R5 springback values (a). Cross-Section 1 (b). Cross-Section 2

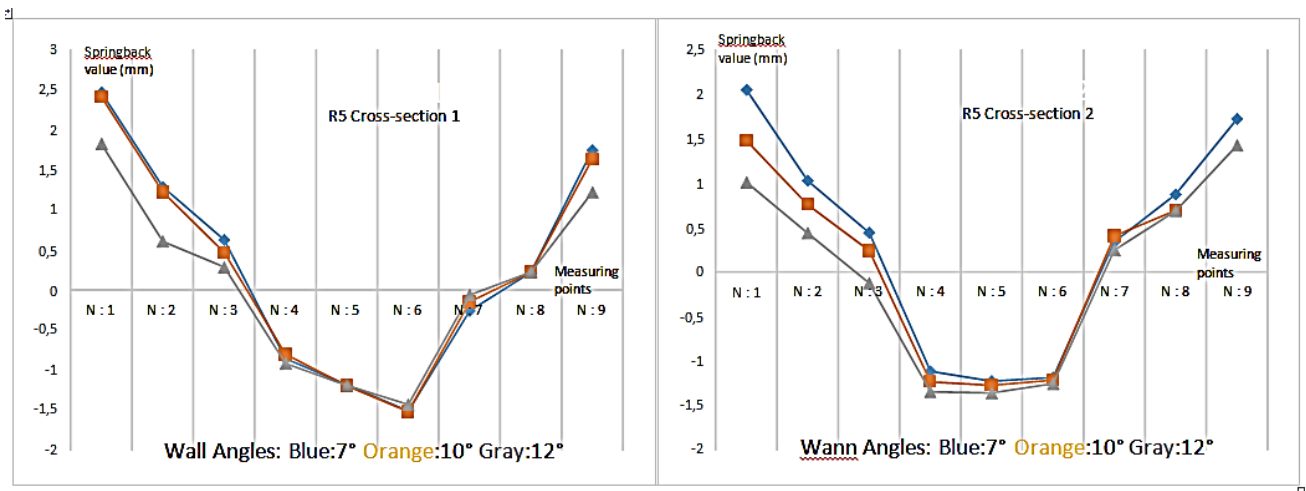
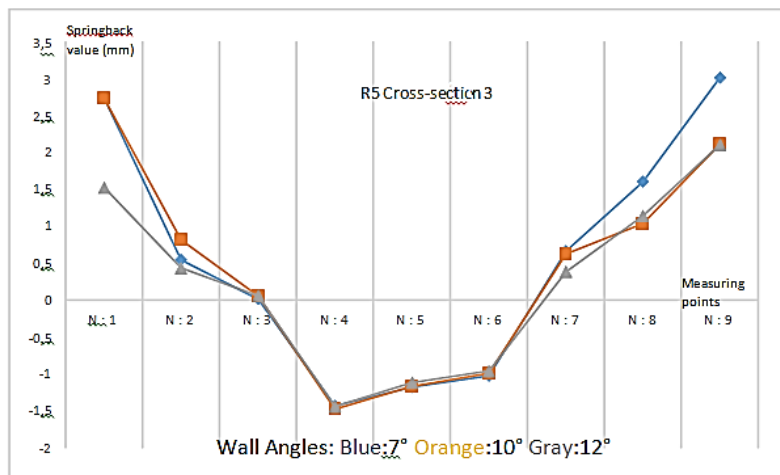


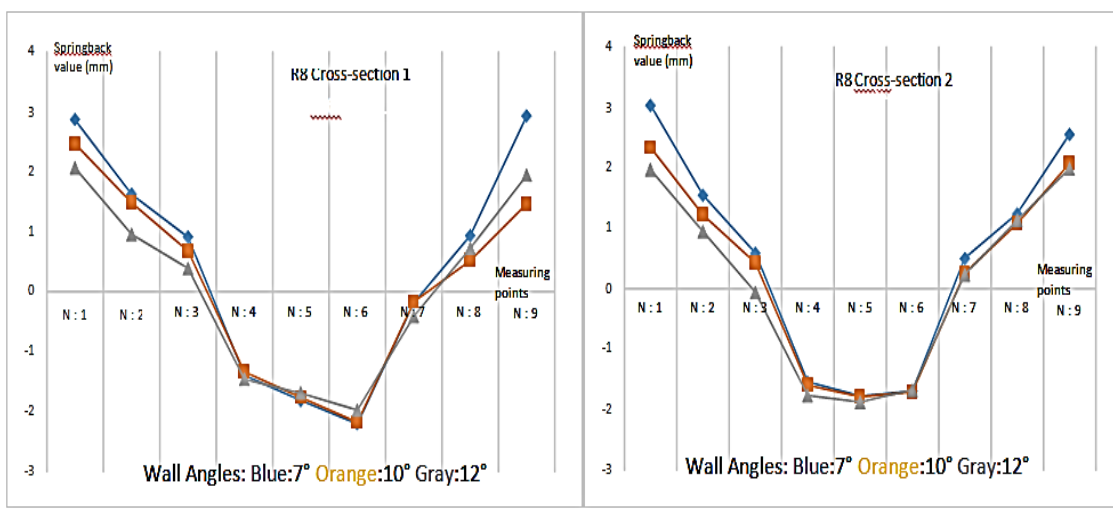
Figure 24. Die radius R5 springback values cross-section 3.



According to the Cross-Section 1 graph, the springback values in cross-section 1 in R8 die radius were examined. When the springback value in N1 was examined, it was found that the springback value decreased by 39% when the wall angle increased from 7° to 12°. The springback values in cross-section 1 also decreased with the increase of the wall angle at other points. Negative springbacks were observed at all wall angles at points N4, N5, N6, springback values were nearly equal. When the springback value in N9 was examined, it was found that the springback value decreased by 50% when the wall angle increased from 7° to 12° Figure 25(a).

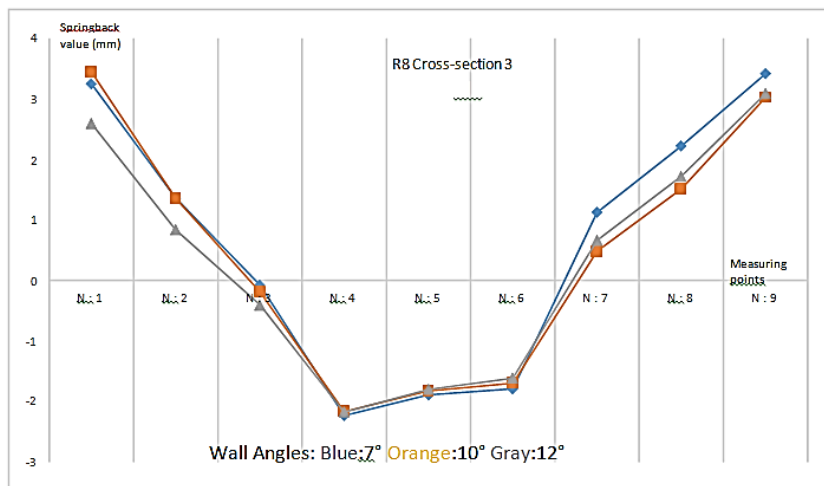
According to the Cross-Section 2 graph, the springback values in cross-section 2 in R8 die radius were examined. When the springback value in N1 was examined, it was found that the springback value decreased by 54,1% when the wall angle increased from 7° to 12°. The springback values in cross-section 2 also decreased with the increase of the wall angle at other points. Negative springbacks were observed at all wall angles at points N4, N5, N6, springback values were nearly equal. When the springback value in N9 was examined, it was found that the springback value decreased by 28.4% when the wall angle increased from 7° to 12° Figure 25(b).

Figure 25. Die radius R8 springback values (a). Cross-Section 1 (b). Cross-Section 2.



According to the cross-section 3 graph, spring-back values in section 3 were examined in the R8 die radius. When the springback value in N1 was examined, it was found that the springback value decreased by 25,2% when the wall angle increased from 7° to 12°. The springback values in cross-section 3 also decreased with the increase of the wall angle at other points. Negative springbacks were observed at all wall angles at points N4, N5, N6, springback values were nearly equal. When the springback value in N9 was examined, it was found that the springback value decreased by 10.6% when the wall angle increased from 7° to 12°. The springback values were found to be high at the points on the far ends of the base Figure 26.

Figure 26. Die radius R8 springback values cross-section 3.



### CONCLUSION

It was observed that successful results were obtained in springback estimations with the correct definition of material and process parameters in finite element studies. In conclusion, by using proper compensation values trial-and-error periods are shortened and die spotting costs are prevented. It was found from the literature researches that the biggest problem in high strength sheet forming is springback. Setting the proper forming parameters with finite element analysis studies will save time in feasibility studies for designers.

Springback measurement values for the U-channel part are shown in Table 7. Measurements were carried out on 3 sections and 9 points in total (Figures 12 and 13). Upon the completion of simulations, after the part was formed as seen in Figure 14, springback values on section 3 of the final part were compared. The die designs were made with Catia, finite element analyses were made with autoform software. When we examine the analysis results, we can see that the wall angles and the die radii are important factors for the springback of the part. In particular, due to high yield and tensile strength of multi-phase high strength sheet, springback values were observed to be high.

When the results of finite elements analysis were examined,

- When the tensile test results are examined; It has been observed that SCGADUB1180 high strength sheet has low elongation values despite high yield and tensile strength values. Close yield and tensile strength values were obtained in all three rolling directions. The elongation values in the 45° rolling direction are lower than in the 0° and 90° rolling directions. When we examine the microstructure of the SCGADUB1180 material, it is seen that it has a high martensite structure. Martensite structure causes deformation hardening. The yield strength increases with strain hardening. High yield stress appears as a reason that increases springback.
- the springback values were examined when the wall angles were 7°, 10°, 12°, it was found that when the process inputs were kept constant in all 3 sections and only the die radius increased from R3 to R8, the springback values in all three wall angles increased with the increase of the die radius. In particular, negative springbacks were observed in the roof of the part. As the die radius increased in all three wall angles, negative springbacks were observed at points N4, N5, N6.
- When the die radii were R3, R5 and R8, and other process inputs were kept constant and the wall angle increased from 7° to 12°, the springback values decreased in all three sections. When the die

radii were R5 and R8, and the wall angles were 7°, 10°, 12°, it was found that negative springback values at points N4, N5, N6 were nearly equal.

- If small tool radii and large wall angles are provided during the design phase of the products where high-strength sheets are used would cause the springback values to be lower. In this way, compensation times and feasibility times will be minimized.

## REFERENCES

1. Şen M, et al. Determination of bend radius based on sheet thickness to optimizing spring-back in the design of automotive sheet metal parts made of bi-phase steels. *Material Sciences*. 2015;12:75-95.
2. Silva CRM, et al. Investigations on the edge crack defect in dual phase steel stamping process. *Procedia Manuf*. 2018;17:737-745.
3. Tisza M, et al. Comparative study of the application of steels and aluminium in lightweight production of automotive parts. *Int J Light Mater Manuf*. 2018;1:229-238.
4. Gomes T, et al. Reducing the simulation cost on dual-phase steel stamping process. *Procedia Manuf*. 2017;11:474-481.
5. Radonjic R, et al. New process design for reduction of springback by forming with alternating blank draw-in. *Procedia Manuf*. 2019;29:217-224.
6. Hattalli VL, et al. Sheet metal forming processes-recent technological advances. *Mater Today Proc*. 2018;5: 2564-2574.
7. Sulaiman S, et al. Springback behaviour in sheet metal forming for automotive door. *AASRI Procedia*. 2012;3:224-229.
8. Sigvant M, et al. Friction in sheet metal forming: Influence of surface roughness and strain rate on sheet metal forming simulation results. *Procedia Manuf*. 2019;29:512-519.
9. Tang L, et al. Advanced high strength steel springback optimization by projection-based heuristic global search algorithm. *Mater Des*. 2013;43:426-437.
10. Pilthammar J, et al. Introduction of elastic die deformations in sheet metal forming simulations. *Int J Solids Struct*. 2018;151:76-90.
11. Aslan Y, et al. V Bükmede Geri Esneme Davranışları. *Gazi University Journal of Science Part C: Design and Technol*. 2014; 2:255-263.
12. Esener E, et al. Sac Metal Şekillendirme prosesinde deneysel tasarım yöntemi ile parametre hassasiyet analizi. *makina imalat teknol. Kongresi 06-07 Aralık 2013*:2-8.
13. Çavuşoğlu O, et al. Deformasyon hızının DP600 ve DP780 sac malzemelerin mekanik özelliklerine ve derin çekme işlemine etkilerinin incelenmesi. *J Fac Eng Archit Gazi Univ*. 2014;29:777-784.
14. Suttner S, et al. Cross-profile deep drawing of magnesium alloy AZ31 sheet metal for springback analysis under various temperatures. *Procedia Manuf*. 2019;29:406-411.
15. Kayabaşı O. A novel design to minimize springback, wrinkling and thickness reduction problem in sheet metal forming process using probabilistic approach. *J Eng Des*. 2020;8:198-209.
16. Peixinho N, et al. Development of forming tool concept validator with variable stiffness blank-holder for high strength steel applications. *Int J Light Mater Manuf*. 2019; 2:116-122.

17. Hou Y, et al. Springback prediction of sheet metals using improved material models. *Procedia Eng.* 2017;207: 173-178.
18. Tisza M, et al. Springback analysis of high strength dual-phase steels. *Procedia Eng.* 2014; 81:975-980.
19. Galdos L, et al. Numerical simulation of U-Drawing test of Fortiform 1050 steel using different material models. *Procedia Eng.* 2017;207:137-142.
20. Konzack S, et al. Prediction and reduction of springback in 3D hat shape forming of AHSS. *Procedia Manuf.* 2018;15: 660-667.
21. Gürsoy OK, et al. Evaluation of the effect of material models on sheet metal finite element analysis forecast performance. *Bilecik Seyh Edebali Univ J of Sci.* 2019;6:1-11.
22. Karabulut S, et al. Üçüncü Nesil Çeliklerin Otomotiv Tasarımında Kullanımı. *Mühendis ve Makina.* 2019:35-39.
23. Esener E. Determination of the hardening effect in plasticity models by finite element analysis. *Dicle Üniv Müh Fakül Mühendi Dergisi.* 2018;11:171-181.
24. Aydın K, et al. DP600 ve HSLA300 Sac Malzemelerde Geri Esneme Davranışlarına Proses Parametrelerinin Etkisinin Deneysel Araştırılması. *Duzce Univ J of Sci and Technol.* 2019; 7:1456-1465.
25. Tuyan M, et al. Sac Kalıplama Prosesinde DD13 ve S355MC Malzemelerin Yırılma Probleminin İncelenmesi ve Çözümü. *Eur j sci tech.* 2020;20:872-880.
26. Aydın H, et al. Otomotiv endüstrisinde kullanılan DP450 ve DP800 saclarında deformasyon hızının ve haddeleme yönünün çekme özelliklerine etkisi. *Balıkesir Üniversitesi Fen Bilim Enstitüsü Derg.* 2019;21;1:323-335.
27. Billur E, et al. Geliştirilmiş Yüksek Mukavemetli Çeliklerin Servo Pres Kullanılarak Bükülmesi. *Makina Tasarım ve İmalat Derg.* 2016;14: 69-76.
28. İriç D, et al. Sac şekillendirme prosesinde kullanılan süzdürme çubuğu frenleme kuvvetinin modellenmesi. *Sak Üniversitesi Fen Bilim Derg.* 2013;17:201-205.
29. Özdemir AO, et al. Investigation of the effect of alloying elements on forming in steel sheets used in the automotive industry. *Gazi Üniversitesi Fen Bilim Derg.* 2017;5:109-119.
30. Kalkan H, et al. Investigation of Friction in sheet metal forming process. *Makina Tasarım ve İmalat Derg.* 2016; 14:88-94.
31. Kılıç S, et al. Ticari TWIP900 ve DP600 yüksek mukavemetli çeliklerin otomotiv endüstrisindeki performanslarının karşılaştırılması. *mühendislik mimar. Fakültesi Derg.* 2016;31:567-578.
32. Taşdemir V. Derin çekme işlemi üzerine kalıp geometrisinin etkisinin sonlu elemanlar analizi. *KSU Mühendislik Bilim Derg.* 2013;16:43-47.
33. Özdemir M, et al. Farklı Isıl İşlemlerinin  $^{16}\text{Mo}_3$  ( 1.5415 ) Sac Malzemelerinin İleri-Geri Esneme Miktarına Etkisinin Deneysel ve Mikroyapısal Olarak İncelenmesi. *ISITES 2014 Karabük.* 2014:148-155.
34. Özcan AG, et al. Yüksek Mukavemetli Çelik Sacların Kaynaklanabilirliği Ve Direnç Spot Kaynağı Parametrelerinin Taguchi Metoduyla Optimizasyonu. *Uludağ Üniversitesi Mühendislik Fakültesi Derg.* 2018;23:333-350.
35. Billur E, et al. New generation advanced high strength steels: Developments, trends and constraints. *Int J Sci Technol Res.* 2016;2:50-62.

36. Kılıçlı V. et al. Nano Beynitik Çelikler. Politek Derg. 2016;19:115-128.
37. Aljibori HSS, et al. Finite element analysis of sheet metal forming process. Eur J Sci Res. 2009;33:57-69.
38. Jadhav S, et al. Applications of finite element simulation in the development of advanced sheet metal forming processes. Berg Huettenmaenn Monatsh. 2018;163:109-118.
39. Esener E, et al. Springback compensation in sheet metal forming processes. 7. Otomotiv Teknol. Kongresi. 2014:1-5.
40. Sayın L, et al. Bakır Sac Levhaların 'V' Bükme Yöntemi İle Şekillendirilmesiyle Oluşan Geri Esneme Miktarının Deneysel Olarak İncelenmesi. Uluslararası Teknol Bilim Derg. 2019;11:147-154.
41. Çetin B, et al. Yüksek Dayanımlı Çelikler in Bükümünde Geri Esneme Açısının Görüntü İşleme ile Belirlenmesi. Makina Tasarım ve İmalat Derg. 2019;17:16-20.